Available online at www.sciencedirect.com
SCIENCE DIRECT®
Physica A 367 (2006) 145–157
PHYSICA A
www.elsevier.com/locate/physa

Chaos synchronization in a lattice of piecewise linear maps with regular and random couplings

A.M. dos Santos[a,*], R.L. Viana[a], S.R. Lopes[a], S.E. de S. Pinto[b], A.M. Batista[b]

[a]*Departamento de Física, Universidade Federal do Paraná 81531-990, Curitiba, Paraná, Brazil*
[b]*Departamento de Matemática e Estatística, Universidade Estadual de Ponta Grossa 84033-240, Ponta Grossa, Paraná, Brazil*

Received 5 September 2005; received in revised form 11 November 2005
Available online 9 December 2005

Abstract

We investigate aspects of the spatio-temporal dynamics exhibited by a one-dimensional lattice of chaotic piecewise linear maps in a coupling prescription which includes both regular (nearest and next-to-nearest neighbors) and randomly chosen couplings. We discuss the conditions for the existence of chaotic synchronized states, and relate them to the coupling parameters. The transition to synchronized behavior is described, and we explore some statistical properties of the time it takes to achieve this regime.

Keywords: Synchronization of chaos; Small world; Coupled map lattices

1. Introduction

Coupled map lattices have been widely recognized as useful models for spatially extended dynamical systems. They present discretized space and time, whereas retaining a continuous state variable whose evolution is governed by a map [1]. In this way coupled map lattices have advantages over cellular automata, in that the former are able to generate local information and a rich spatio-temporal dynamics [2]. Most research done on coupled map lattices has focused on limiting cases of coupling: the so-called local, or Laplacian case takes into account the effects of only the nearest neighbors of a given lattice site [3]; whereas in the global case each map interacts with the "mean-field" generated by all lattice sites [4]. Recently, a form of coupling was proposed which considers the effect of all neighbors decreasing as a power-law with the lattice distance, and which reduces to the above mentioned coupling prescriptions as limiting cases [5].

Another classification of these systems comprises regular lattices, for which there is a kind of translational symmetry of the coupling term; and random lattices, which exhibits shortcuts between sites (not necessarily close to each other) randomly chosen according to a specified probability distribution. Recent investigations in lattice models of sociological interest, like the so-called small-world phenomenon, have raised the need of lattices which share properties of both regular and random lattices [6]. In regular lattices, the

*Corresponding author.
E-mail address: ansantos@fisica.ufpr.br (A.M. dos Santos).

0378-4371/$ - see front matter © 2005 Elsevier B.V. All rights reserved.
doi:10.1016/j.physa.2005.11.012

existence of interactions with the nearest neighbors of a given site leads to a modeling difficulty, in that the transmission velocity of signals is limited by the diffusive nature of the coupling. By way of contrast, many interesting models require the introduction of shortcuts for rapid signal propagation (like in epidemiological models for spread of infections or in models for propagation of gossips in social networks) [7].

Purely random lattices present a very small amount of clustering, which can be described as the property that, if two given sites are connected to a third one, hence these sites are also connected to each other. Some amount of clustering is highly desirable in models of social and epidemiological networks. On the other hand, regular lattices typically show a high level of clustering.

The quest for lattices with small average distance between sites, yet with a reasonably large degree of clustering has led to the introduction of models with both regular and random interactions [6,7]. The properties of such small-world lattices have been studied with respect to some aspects of their spatio-temporal dynamics, with special emphasis on synchronization [8]. The synchronization properties of any lattice are enhanced with the addition of the randomly chosen shortcuts, which is revealed by a variety of numerical diagnostics. Chaos synchronization is particularly interesting to investigate, since it depends in an intricate fashion on the dynamical properties of the coupled map lattice. The existence of chaos synchronization of small-world networks has been shown for a general class of such lattices [9–11].

The dynamical properties of the synchronized state in lattices with random nonlocal connectivity were investigated by Chaté and Manneville [12] and Gade [13]. In this paper, we aim to focus on a hitherto not completely understood issue, i.e., the dependence of the chaos synchronization of the lattice on the coupling parameters, when both local and nonlocal connections are present. The transition from non-synchronized to synchronized behavior is investigated by means of an order parameter that presents a sharp transition curve, relating the critical coupling strength for achieving synchronization with the probability of random shortcuts. Moreover, we investigate the time it takes to achieve a chaotic synchronized state, which is also a useful measure of how the introduction of random couplings helps to improve synchronization in the lattice system. We remark that the introduction of long range shortcuts is not the only way to induce chaotic synchronization in a locally coupled lattice: it can also be done by the introduction of a time delay in the couplings [14], and the addition of an external forcing [15].

This paper is organized as follows: in Section 2, we introduce a lattice with regular and random couplings and investigate the characterization of spatial patterns, focusing on synchronization of chaotic maps and its numerical detection. In Section 3, we investigate some dynamical properties of the synchronized state and their dependence with the coupling parameters. The numerical results are explained from the stability properties in the directions transversal to the synchronized manifold in the system phase space. Our conclusions are left to the last section.

2. Lattice spatio-temporal dynamics

Let us consider a lattice of N maps, each of them with its state variable at discrete time $n: x_n^{(i)}$, where $i = 1, 2, \ldots N$. A model presenting regular as well as random couplings is

$$x_{n+1}^{(i)} = (1-\varepsilon) f(x_n^{(i)}) + \frac{\varepsilon}{4+M}\left[f(x_n^{(i-1)}) + f(x_n^{(i-2)}) + f(x_n^{(i+1)}) + f(x_n^{(i+2)}) + \sum_{j=1}^{N} f(x_n^{(j)}) I_{ij} \right], \tag{1}$$

where $\varepsilon > 0$ is the coupling strength, and the local dynamics at each site is represented by a piecewise linear map $x \mapsto f(x) = \beta x \pmod 1$. For $\beta > 1$ the map displays strong chaos, with Lyapunov exponent $\lambda_U = \ln \beta$ (from now on we choose $\beta = 3$).

This coupling scheme has two contributions: a regular one, from the nearest and second-nearest neighbors to a given site; and a random term represented by the matrix elements I_{ij}. We introduce a fixed number M of randomly chosen shortcuts for each site, with uniform probability $p = M/N$. Hence, in each row of the $N \times N$ connectivity matrix I_{ij} there are M randomly-chosen entries equal to 1, the $N - M$ others being padded with

zeroes. As a consequence, for every $i = 1, 2, \ldots, N$, we have

$$\sum_{j=1}^{N} I_{ij} = M = Np. \tag{2}$$

We have computed the Lyapunov spectrum of the system given by Eq. (1), in order to assure the chaoticity of the coupled map lattice for the coupling parameter values treated in this work. As a general rule, the number of positive Lyapunov exponents of the lattice decreases with the probability of nonlocal shortcuts p, for a given value of the coupling strength ε, until, for a critical ε-dependent value, it reduces to just one positive exponent. This strongly suggests that the coupled map lattice has achieved a state for which all the maps are completely synchronized, $x_n^{(1)} = x_n^{(2)} = \cdots x_n^{(N)}$, undergoing identical chaotic dynamics.

A diagnostic of complete synchronization is the complex order parameter introduced by Kuramoto [16]

$$z_n = R_n \exp(i\varphi_n) \equiv \frac{1}{N} \sum_{j=1}^{N} \exp(2\pi i x_n^{(j)}), \tag{3}$$

where R_n and φ_n are the amplitude and angle, respectively, of a centroid phase vector for a one-dimensional lattice with periodic boundary conditions. In the following, we shall consider lattices with $N = 3000$ sites with periodic boundary conditions: $x_n^{(i)} = x_n^{(i\pm N)}$ and initial conditions $x_0^{(i)}$ randomly chosen within the interval $[0, 1]$ according to a uniform distribution. If lattices with a smaller number of sites are chosen, the numerical results turn out to depend heavily on the initial conditions. Our choice of N has proven to be good enough to yield results which, to a large extent, do not depend on the specific profile we choose for the initial conditions. Moreover, Li and Chen [10] have argued that simulations of small-world networks are good as long $pN = M > 1$, which will be always the case in this paper.

For uncoupled maps, we would expect patterns for which the site amplitudes $x_n^{(j)}$ would be spatially uncorrelated that their contribution to the result of the sum in Eq. (3) is typically small. In particular, for a uniform distribution of $x_n^{(i)}$ the order parameter magnitude is zero. By way of contrast, in a completely synchronized state the order parameter magnitude rapidly tends to 1, indicating a coherent superposition of the phase vectors for all sites with the same amplitudes at each time. Fig. 1 depicts the time-averaged order parameter magnitude

$$\bar{R} = \lim_{T\to\infty} \frac{1}{T} \sum_{n=m}^{T} R_n \tag{4}$$

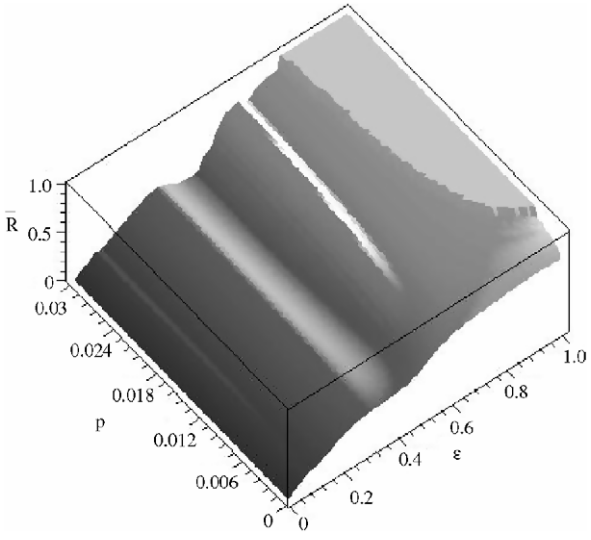

Fig. 1. Time-averaged order parameter as a function of the probability of random shortcuts p and the coupling strength ε.

as a function of the probability of random shortcuts p and the coupling strength ε, where m is the number of transient iterations discarded. If $p = 0$ we do not have any shortcuts and the lattice is purely regular. The average order parameter is less than 1, denoting a non-synchronized state. In fact, locally coupled lattices of chaotic maps are known to be very hard to synchronize, even for large coupling strengths, since the diffusive effect of coupling is too weak to overcome the intrinsic chaotic behavior displayed by individual maps. In Fig. 1 we focus on ε_c, which is the less value of the coupling strength for which the lattice synchronizes; p_c having a similar meaning for the shortcut probability.

Accordingly, we expect to see chaos synchronization only if nonlocal interactions take place. This can be achieved, for example, if the coupling intensity decays with the distance along the lattice in a power-law fashion. In our case, however, it suffices to include a small number of shortcuts linking non-neighboring sites. Fixing ε at a constant value, say $\varepsilon = 0.78$, and for p growing from zero to $p_c \approx 0.025$ we observe in Fig. 1 an overall increase of the order parameter magnitude, showing the formation of an increasingly large number of synchronization plateaus along the lattice.

For p approaching $p_c \approx 0.03$ the order parameter becomes constant and equal to the unity, which characterizes a completely synchronized state. The critical value p_c for which this transition occurs depends on the coupling strength ε. It initially is lowered from $p \approx 0.03$ (for small ε) but saturates at $p \approx 0.005$ for stronger coupling. It is instructive to perform a two-dimensional cross-section of Fig. 1 showing more clearly the completely synchronized ($\bar{R} = 1$) and non-synchronized ($\bar{R} \neq 1$) regimes (Fig. 2). These two phases are separated by a transition curve of critical points (ε_c, p_c) in the parameter plane. Our numerical results in the probability range $[0, 0.03]$ can be fitted by the following expression:

$$\varepsilon_c = \frac{A}{p_c} + B, \tag{5}$$

where $A = 1.20 \times 10^{-3}$ and $B = 0.727$.

For example, when $\varepsilon = 1.0$, there follows that the critical probability for synchronization is $p_c = 4.39 \times 10^{-3}$. On the other hand, if p is large enough we expect to recover at least some of the properties held by a globally coupled lattice, since the number of shortcuts *per* site is limited to N. In such an extreme case, we would have the equivalent of a regular lattice with global "mean-field" coupling type, for which each site interacts with all its other neighbors, irrespective of their position along the lattice.

The nature of the transition towards a synchronized regime can be grasped by considering the spatio-temporal patterns of the coupled map lattice in the vicinity of the transition curve $\varepsilon_c(p_c)$ in Fig. 2. Let us take

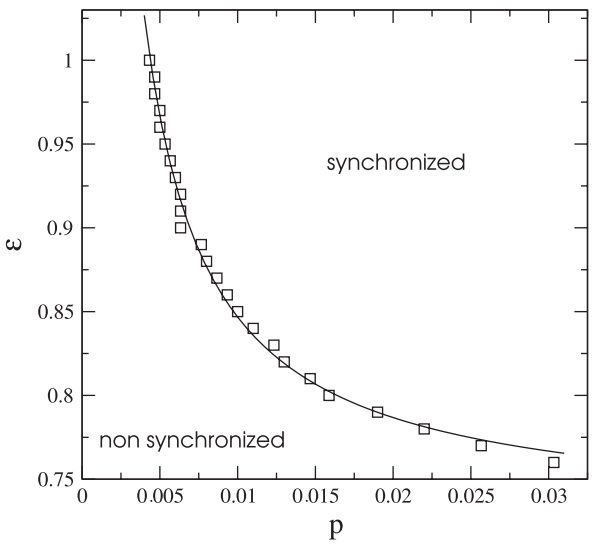

Fig. 2. Completely synchronized and non-synchronized phases of the coupled map lattice versus the coupling parameters. The squares stand for numerical simulations, and the full line is the nonlinear fit given by Eq. (5).

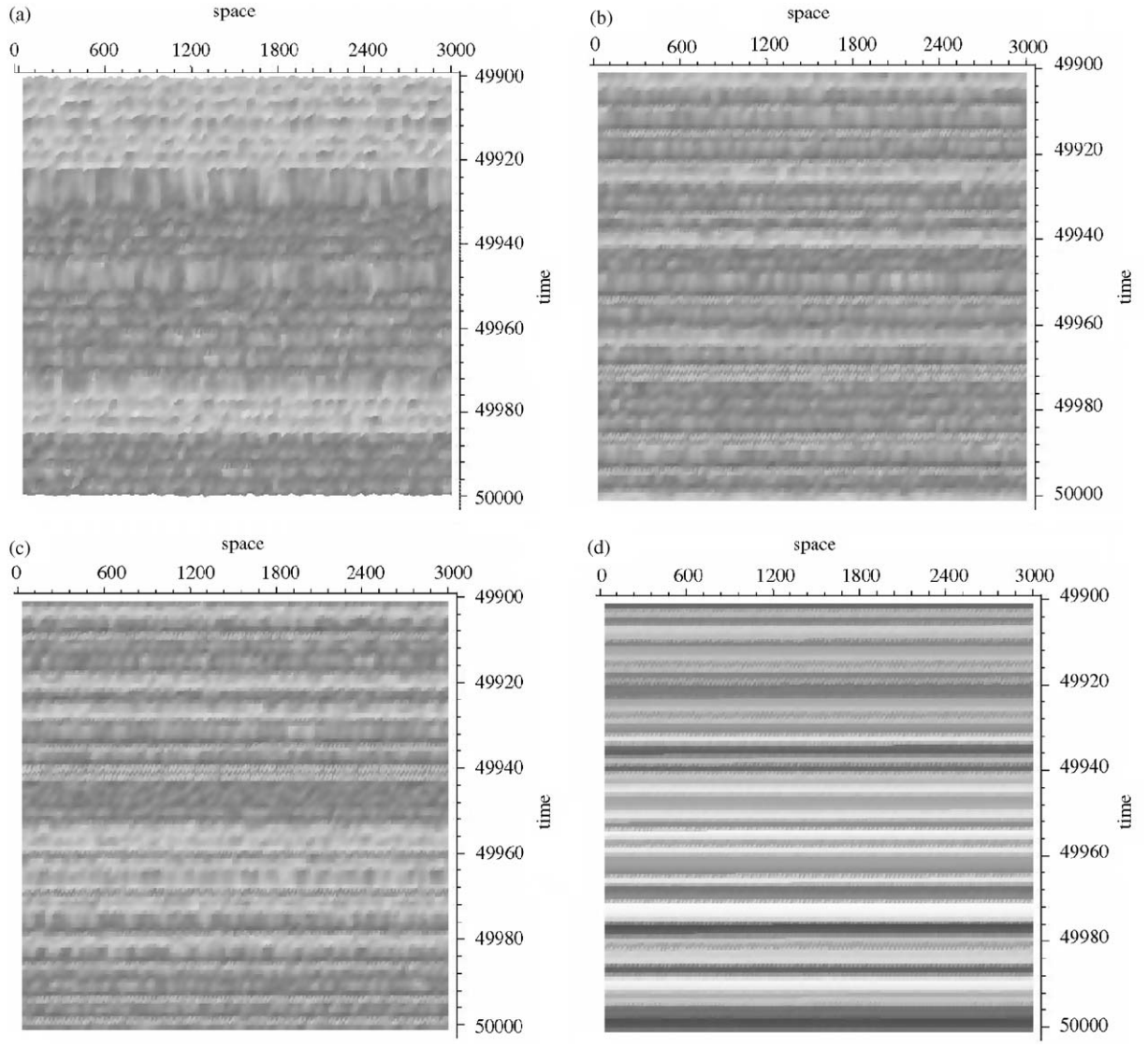

Fig. 3. Space–time-amplitude patterns for: (a) $\varepsilon = 0.85$ and $p = 5.0 \times 10^{-3}$; (b) 9.0×10^{-3}; (c) 9.3×10^{-3}; (d) $10.0 \times 10^{-3} \approx p_c$.

the coupling strength at a fixed value, say $\varepsilon = 0.85$, and vary the shortcut probability in the vicinity of the critical value $p_c \approx 0.01$. In order to facilitate visualization of the spatial patterns during a time-100 interval sampled after $n = 49,900$ iterations, when we expect all transients to be already died out, in Fig. 3 we depict space–time plots where the amplitudes $x_n^{(i)}$ are represented in a greyscale, and for which synchronized plateaus appear as spatially homogeneous clusters.

For p much more smaller than p_c [Fig. 3(a)], we do not observe much spatial coherence between sites, as expected from a non-synchronized state. Increasing the number of shortcuts [$M = 27$ out of $N = 3000$ sites, cf. Fig. 3(b)] synchronization plateaus begin to be clearly visible for many times. They appear alternately with non-synchronized regions, characterizing an intermittency between the two regimes. Some plateaus span the entire lattice, whereas other plateaus represent limited domains of spatial coherence, separated by "defects" of spatial disorder.

The completely synchronized state is lost, when the coupling strength, or the shortcut probability p are decreased past their critical values, through an intermittent transition in spatial and temporal scales.

The completely synchronized state breaks down into a number of clusters with different lengths. A crude estimation made on Fig. 3(b) gives 17 such coherent structures distributed during 100 time units. These facts suggest a scenario of spatio-temporal intermittency, which is characterized by the coexistence of laminar regions, which exhibit regular dynamics both in space and time, and spatially irregular bursts with temporal chaotic dynamics, and which is often related to the transition to fully turbulent states in continuous systems like fluids [17].

Adding just one more shortcut *per* site to the lattice leads us to approach the criticality at $p = p_c$ [Fig. 3(c)], and the widths and the number of spatially coherent clusters increase, indicating that the synchronized regions are longer and more frequent than before. We could say that the average cluster length would increase with p and actually diverge as p goes to p_c. Afterwards, [Fig. 3(d), obtained by adding just two more shortcuts *per* site to the previous case] we nearly observed only synchronized chaotic dynamics. It is thus remarkable to see the effect of just one randomly chosen shortcut *per* site (in a lattice with out 3000 maps) in terms of the ability of the system to achieve a stationary synchronized state. We have also done numerical simulations with lattices of smaller size, and found that the critical values of ε and p necessary for the transition to a non-synchronized state are slightly changed such that the border of the synchronization region in Fig. 1 is displaced upwards.

We stress that a phase transition curve similar to that depicted in Fig. 2 exists for power-law couplings, for which the lattices are purely regular, but where the role of the shortcut probability would be played by the effective range of the interaction [18,19]. In such couplings, the interaction strength decreases with the lattice distance as a power-law

$$x_{n+1}^{(i)} = (1-\varepsilon) f(x_n^{(i)}) + \frac{\varepsilon}{\eta(\alpha)} \sum_{j=1}^{N'} \frac{1}{j^{\alpha}} [f(x_n^{(i+j)}) + f(x_n^{(i-j)})], \tag{6}$$

where $\alpha > 0$ is a range parameter, and $\eta(\alpha) = 2\sum_{j=1}^{N'} j^{-\alpha}$, with $N' = (N-1)/2$, for N odd. When α goes to infinity, the only contributions to the coupling are from the nearest-neighbor sites, such that Eq. (6) reduces to the local diffusive-type prescription

$$x_{n+1}^{(i)} = (1-\varepsilon) f(x_n^{(i)}) + \frac{\varepsilon}{2} [f(x_n^{(i+1)}) + f(x_n^{(i-1)})]. \tag{7}$$

On the other hand, when $\alpha = 0$ the contributions of all sites are equally important regardless of their positions along the lattice, such that the coupling reduces to a global mean-field coupling.

$$x_{n+1}^{(i)} = (1-\varepsilon) f(x_n^{(i)}) + \frac{\varepsilon}{N-1} \sum_{j=1, j\neq i}^{N} f(x_n^{(j)}). \tag{8}$$

We argue that coupled map lattices of the type treated in this paper, in which there are regular and random connections, exhibit, in the large-p limit, properties similar to those of globally coupled lattices (i.e., when $\alpha = 0$). The mean-field coupling prescription, Eq. (8), could also be obtained by our coupling map lattice, Eq. (1), in the limit when the interaction matrix I_{ij} has all its entries equal to the unity, i.e., $M = N$, what gives $p = M/N = 1$. A manifestation of that analogy is that, while spectrum of Lyapunov exponents for a globally coupled lattice as Eq. (8) has been proved to exhibit a transition to low-dimensional chaos at a critical value of $\varepsilon_c = 2/3$ [18], we found a similar transition for our lattice, when p is comparatively large, at a value around 0.7. On the other hand, when p vanishes, only the nearest and the next-to-the-nearest neighbors will contribute to coupling in Eq. (1), and we obtain essentially the local diffusive coupling form given by Eq. (7). Hence, the shortcut probability plays a role similar to the range parameter, in interpolating between global and local couplings. We stress, however, that this analogy cannot be pushed too far, since the nature of the interactions are quite distinct.

Another quantity one can build with help of the order parameter is its magnitude averaged over a given number N_c of different randomly chosen initial conditions

$$\langle R_n \rangle = \frac{1}{N_c} \sum_{i=1}^{N_c} R_n(x_0^{(i)}), \tag{9}$$

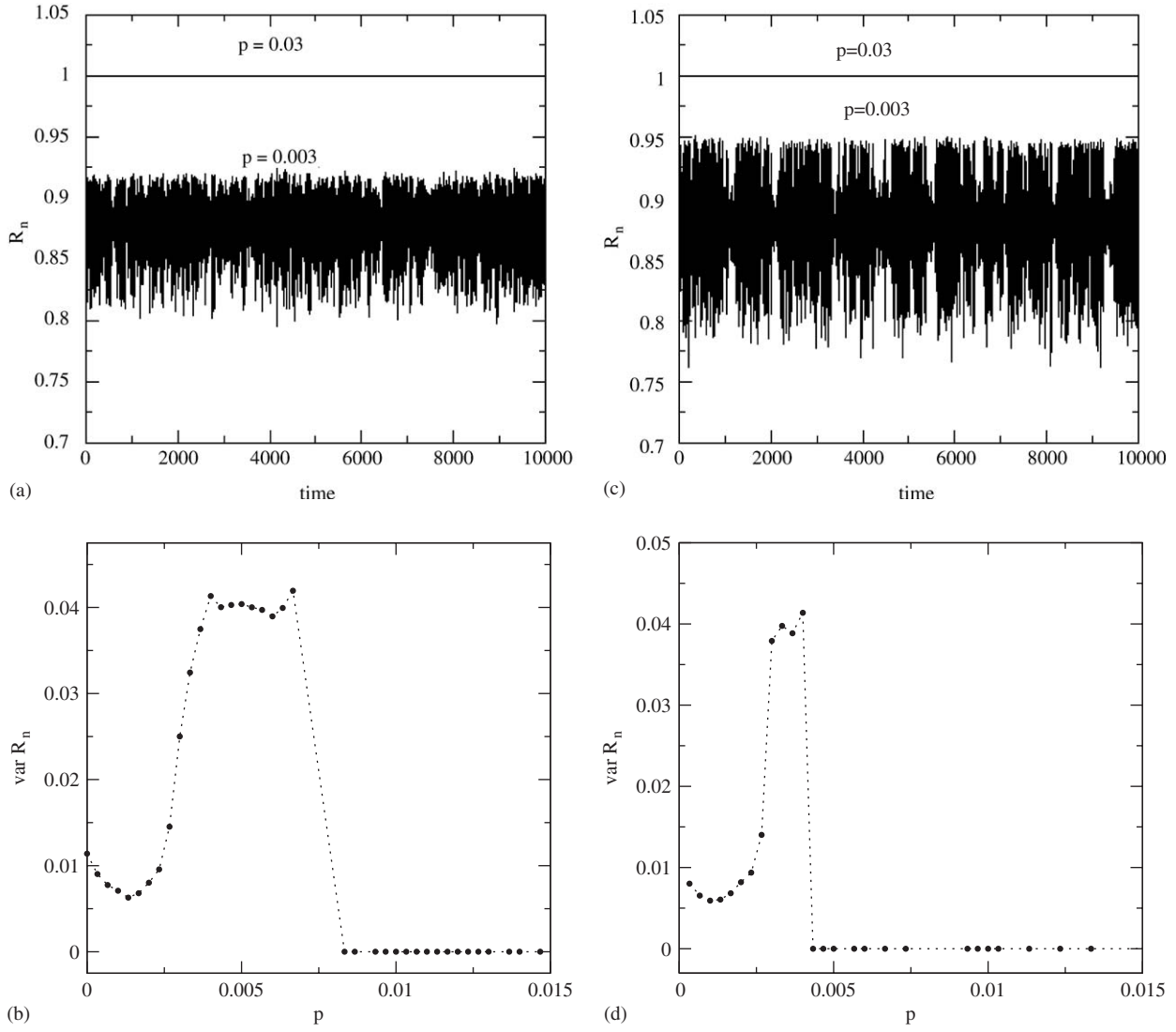

Fig. 4. (a) Order parameter magnitude averaged over 30 randomly chosen initial conditions, as a function of time, for $\varepsilon = 0.9$; (b) variance of the order parameter magnitude fluctuations in terms of shortcut probability; (c) and (d) refer to $\varepsilon = 1.0$.

and which, in general, is not equal to the time average $\bar{R}$ unless the spatio-temporal dynamics is ergodic in both scales.

In Fig. 4(a), we show the time evolution of the mean $\langle R_n \rangle$ for a lattice with 3000 maps, averaging over $N_c = 30$ initial patterns, with $\varepsilon = 0.9$ and two different values for the shortcut probability. Here we meet again the striking influence of even a modest number of random shortcuts: while for $p = 0.003$ the order parameter fluctuates with a characteristic variance $\mathrm{var}(R_n) \approx 0.02$, indicating absence of synchronized behavior, when p increases to 0.03 the order parameter average reaches the unity with a variance less than the numerical accuracy used (viz., $\sim 10^{-12}$). Fig. 4(b) plots the variance $\mathrm{var}(R_n)$ versus the probability p, indicating a clearcut transition to synchronized behavior for $p > p_c \approx 0.008$, in good accordance with the fitted phase transition curve of Fig. 2. The peak observed for the order parameter variance just before the transition is due to an intermittent bursting between synchronized and non-synchronized regimes. These results are not appreciably changed when a slightly higher value of the coupling strength is used [see Figs. 4(c) and (d)], the transition occurring at the corresponding critical value of the shortcut probability p.

3. Stability properties of the synchronization manifold

A geometric way to study synchronization in phase space is to regard a completely synchronized state $x_n^{(1)} = x_n^{(2)} = \cdots x_n^{(N)}$ as defining a one-dimensional synchronization manifold $\mathscr{S}$ belonging to the full N-dimensional phase space of the coupled-map lattice [20]. The dynamics along $\mathscr{S}$ is the same as of an uncoupled chaotic map with a positive Lyapunov exponent. Hence, there are $N-1$ remaining Lyapunov exponents, hereafter referred as transversal ones.

If a completely synchronized state occurs at all, it must be a valid solution of the coupled map lattice given by Eq. (1). This imposes a constraint on the form of the coupling matrix, what can be seen by inserting the common value of all sites at any time, denoted χ, into Eq. (1), there results that the dynamics on the synchronization manifold is given by

$$\chi = (1-\varepsilon)f(\chi) + \frac{\varepsilon}{4+M}\left[4f(\chi) + f(\chi)\sum_{j=1}^{N} I_{ij}\right] = f(\chi), \tag{10}$$

where we used Eq. (2), i.e., provided there are N nonzero entries in each row of the connectivity matrix. If we had relaxed this assumption, a completely synchronized state would be forbidden in this system.

In fact, if all the transversal Lyapunov exponents are negative, then almost all synchronized trajectories in $\mathscr{S}$ are transversely stable. By "almost all" we mean except a Lebesgue measure zero set of unstable periodic orbits embedded in $\mathscr{S}$. There follows that $\mathscr{S}$ is an attractor in the weak Milnor sense [21]. From the practical point of view, however, we have good synchronization properties if, at least locally, $\mathscr{S}$ is an asymptotically stable attractor, which implies that: (i) all trajectories off but close enough to $\mathscr{S}$ asymptote to it; (ii) $\mathscr{S}$ is Lyapunov-stable, i.e., if a trajectory starts close enough to $\mathscr{S}$ it will not go far away from $\mathscr{S}$ [22].

It must be remarked that $\mathscr{S}$ can also be a weak Milnor attractor with an infinite number of unstable periodic orbits with positive transversal Lyapunov exponents. In this case, $\mathscr{S}$ will be no longer Lyapunov-stable, since some trajectories off but close to $\mathscr{S}$ eventually go farther away due to the nonlinearities of the dynamics in the directions transversal to $\mathscr{S}$. This characterizes a locally riddled basin of attraction for the attractor in $\mathscr{S}$ [23]. Such escaping trajectories may have one of the following outcomes: they either converge to $\mathscr{S}$ after a certain (possibly large) time; or they may converge to another attractor off $\mathscr{S}$; and they may not converge at all, producing an intermittent bursting between consecutive regions of approximate synchronization [22]. These behaviors can also be characterized with help of the statistical properties of the finite-time Lyapunov exponents along the directions transversal to $\mathscr{S}$ [19,24].

The time evolution of a coupled lattice towards synchronization is determined by the dynamics in directions transversal to $\mathscr{S}$. It can be tracked down by computing at each discrete time the orthogonal distance i.e., the distance in the plane defined by the orthogonal directions to $\mathscr{S}$ in the N-dimensional phase space between the phase point $(x_n^{(1)}, \ldots, x_n^{(N)})$ and the synchronization manifold

$$d_n^2 = \sum_{j=1}^{N} (x_n^{(j)})^2 - \left(\frac{\sum_{j=1}^{N} x_n^{(j)}}{\sqrt{N}}\right)^2. \tag{11}$$

We can also write this distance as $d_n^2 = N\sigma_n^2$, where

$$\sigma_n^2 = \langle x^2\rangle_n - \langle x\rangle_n^2, \tag{12}$$

is the variance of the map amplitudes ($\mathrm{var}(x_n)$) with respect to their lattice average $\langle x\rangle$ at a given time n. In general, for nearly synchronized states, the order parameter R yields better results than the distance d^2, since the latter fluctuates around zero (due to numerical precision), whereas R goes to unity without noticeable fluctuation. Hence R turns to be a more precise diagnostic of synchronization for such states. On the other hand, for non-synchronized states we found both diagnostics equally accurate.

The analysis of the distance to the synchronization manifold furnishes results complementary to the order parameter introduced in the previous section. As representative examples, we depict in Fig. 5(a) the time series of the distance d_n for two values of the probability p differing by one order of magnitude, when $\varepsilon = 0.9$. When we have a few random shortcuts ($p = 0.003$) this distance oscillates in a rather irregular fashion, whereas an

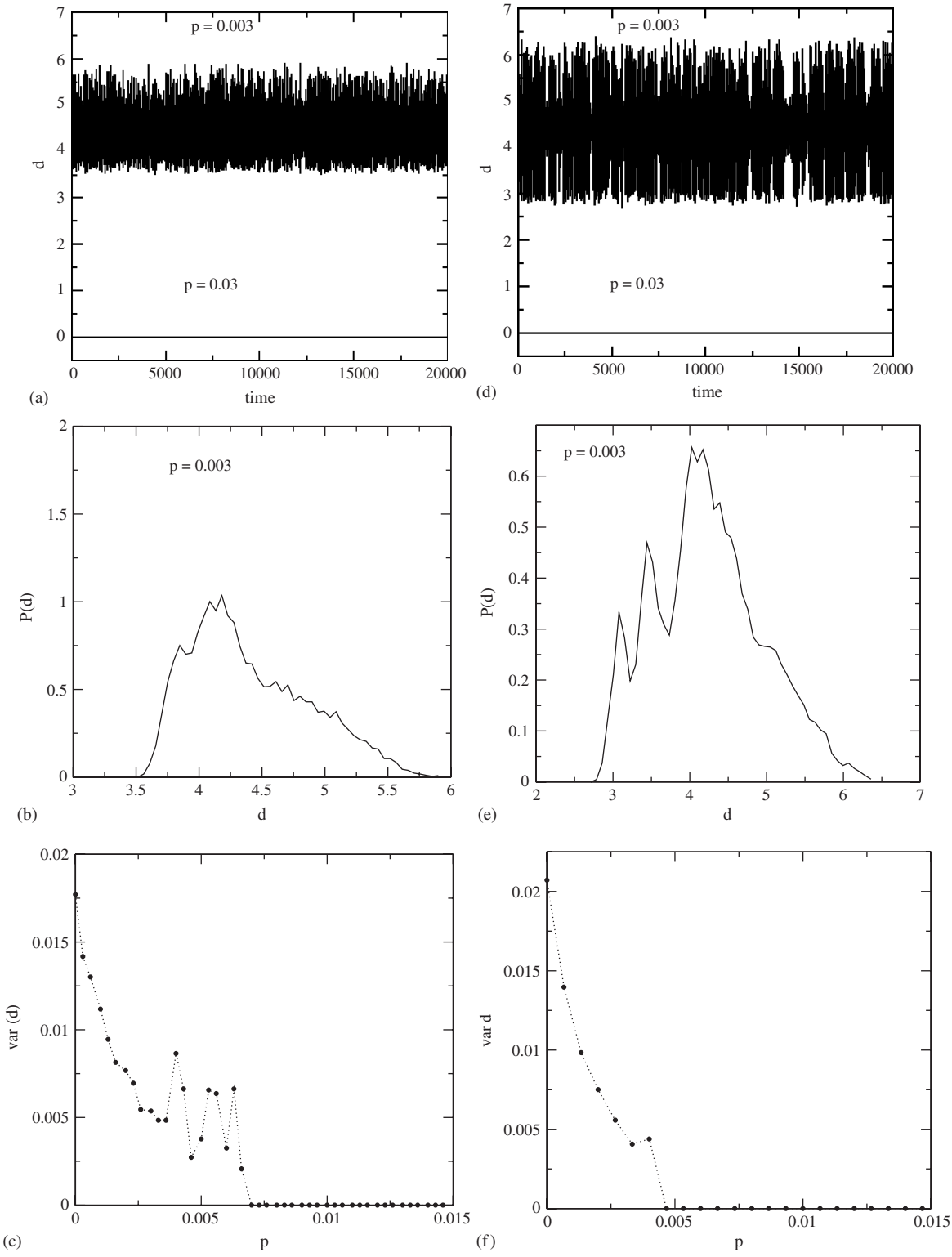

Fig. 5. (a) Distance to the synchronization manifold for $\varepsilon = 0.9$ and two different shortcut probabilities; (b) frequency distribution of the distances for $p = 0.003$; (c) variance of distance oscillations as a function of p; (d), (e) and (f) refer to $\varepsilon = 1.0$.

increased probability ($p = 0.03$) leads the system trajectories to settle down in a synchronization manifold. The variance of such oscillation depends on the shortcut probability [Fig. 5(c)] in the same fashion as the variance of order parameter magnitude [see Fig. 4(b)]. For slightly higher coupling and small p we still see such oscillations [Fig. 5(d)], but with a larger variance [Fig. 5(f)].

The irregular oscillations of d observed for small shortcut probability p have a broad distribution with respect to its mean value, as shown by Figs. 5(b) and (c) for lattices with $\varepsilon = 0.9$ and 1.0, respectively. These oscillations are a characteristic feature of non-synchronized behavior. On the other hand, for higher values of p the chaotic trajectories analyzed converge to $\mathscr{S}$, which is a numerical indication that $\mathscr{S}$ is at least a weak Milnor attractor. As far as our numerical investigation was concerned, however, we did not find any trace of behavior leading to trajectories departing from $\mathscr{S}$ and returning to it in the form of intermittent bursts of non-synchronized behavior. This suggests that the attractor in $\mathscr{S}$ is asymptotically stable, although no rigorous proof of this statement is available for this system in particular.

Once we have reliable ways to assess whether or not the system has reached the synchronization manifold, it is possible to investigate how long does it take for a given initial condition to generate a trajectory converging to a completely synchronized state. In Fig. 6 we plot the time elapsed to reach a synchronized state as a function of the coupling strength, for a single realization with a fixed probability $p = 0.03$. Since the variation shown by Fig. 6 is quite fast over many decades, we used a log–log plot to evidence an initial decrease of the time to synchronize as the coupling becomes stronger. This is an expected feature, since the stronger is the coupling, the easier is for the lattice to synchronize.

Depending on the initial condition chosen, the time it takes to achieve complete synchronization varies according to Fig. 7, where we plot histograms for the relative frequency with which, for fixed coupling parameters (p, ε), we have different times for synchronization. For $p = 0.03$ and $\varepsilon = 1.0$, the majority of initial conditions leads to 35 to 40 iterations to reach a completely synchronized state. However, there are some initial conditions which lead to a surprisingly large time, indicating that in the transversal dynamics to the synchronization manifold there must be invariant structures which act as traps for the non-synchronized trajectories.

Since the dimensionality of the phase space is too high to allow for analytical studies of the transversal dynamics, we can guess some explanations for this effect, based on results valid for similar systems. We can regard the trajectories off the synchronization manifold as chaotic transients, since they resemble truly chaotic trajectories of the system attractor (lying on the synchronization manifold) and belong to its basin of attraction. However, such trajectories eventually converge to the synchronization manifold, provided it is an asymptotically stable attractor.

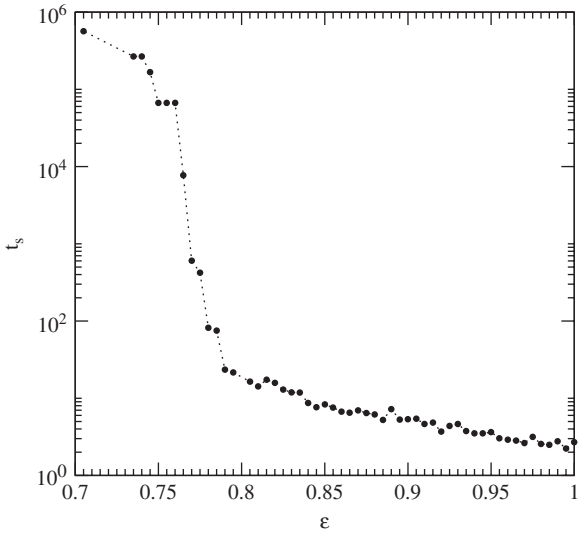

Fig. 6. Time elapsed to reach a synchronized state as a function of the coupling strength, for a fixed probability $p = 0.03$.

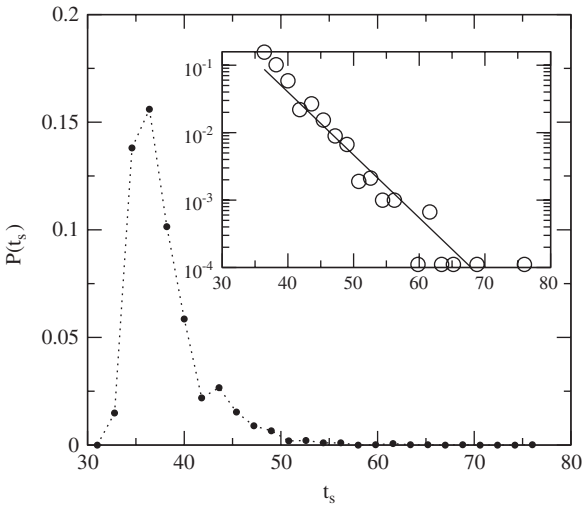

Fig. 7. Probability distribution for the times the coupled-map lattice take for achieve a completely synchronized state. The inset shows a magnification of the decaying part of the distribution, and the full line is an exponential fit to the numerical results (circles).

A common feature of chaotic transients is that they arise from non-attracting and invariant structures called chaotic saddles. A chaotic saddle can be formed, by example, due to a collision between a chaotic attractor and the boundary of its own basin of attraction (boundary crisis) or with an unstable periodic orbit (interior crisis) [25]. In both cases, the structure of the chaotic saddle is comprised by a maze of intersecting stable and unstable manifolds of unstable periodic orbits belonging to the saddle. The set of initial conditions exactly on a chaotic saddle has zero Lebesgue measure, but an initial condition close enough to the saddle may stay there for a large time before escaping from the saddle and being directed to the synchronization manifold.

If this reasoning is applicable to the dynamics transversal to $\mathscr{S}$, it is even possible to give plausibility arguments for the form of the probability distribution depicted in Fig. 7, which exhibits exponential decay (an exponential fitting of numerical results is shown in the inset of Fig. 7). Supposing that the attractor at $\mathscr{S}$ is asymptotically stable, there are just two possible outcomes for a non-synchronized trajectory from an initial condition near the chaotic saddle: it will either converge to the attractor in $\mathscr{S}$; or else it will remain in the immediate vicinity of the chaotic saddle for a long time. However, since the saddle has zero Lebesgue measure in phase space, the probability of escape is much larger than of not doing so for a finite-time (in the infinite-time limit all trajectories will asymptote to $\mathscr{S}$). As a consequence, the escape from the chaotic saddle obeys an exponential decay law.

4. Conclusions

In this paper, we explored some aspects of the spatio-temporal dynamics displayed by a coupled-map lattice with regular and random interactions, inspired by models proposed for describing small-world networks. We stress that the main difference between those earlier models and ours is the presence of constraints in the number of random shortcuts a given site may have, whereas in other small-world models this number may vary from site to site. The main reason to adopt such a constraint is to guarantee the existence of a synchronization manifold in the phase space, where all lattice sites, although chaotic, oscillate in a synchronous fashion. From the practical point of view this would restrict the application of the kind of lattice we are introducing to situations in which the number of nonlocal interactions must be kept fixed by some external rule.

From the dynamical point of view, our numerical results indicate that the chaoticity of the lattice as a whole, as measured by its Lyapunov spectrum, essentially decreases as the number of random shortcuts is increased, indicating that the addition of nonlocal connections to an otherwise locally coupled chaotic lattice has the ability of reduce chaos in the system. For studying the spatial randomness, we used an order parameter

to characterize the existence of completely synchronized chaotic maps, for which the degree of chaoticity decreases, since the dynamics occurs in a low-dimensional manifold of the phase space, all the corresponding transversal directions being attractive. The existence of two phases, synchronized and non-synchronized, was evidenced by means of a phase transition curve very similar to that occurring in regular lattices with nonlocal interactions whose strength diminishes with the lattice distance as a power-law.

The behavior near the transition curve between synchronized and non-synchronized phases has been explored with help of the pointwise distance to the synchronization manifold. Our numerical results support the claim that the chaotic synchronized trajectories are asymptotically stable with respect to perturbations along directions transversal to the synchronized manifold. We found that the time it takes for this distance to vanish, indicating that the lattice eventually synchronizes, decreases exponentially with the strength of the interactions, both regular and random. Accordingly, the statistical distribution of these times can be fitted by an exponential decay law.

In summary, we explored in this paper a kind of coupled-map lattice which can model situations in which there are randomly chosen shortcuts, as in small-world networks, but with a dynamically different behavior, since there is a synchronization manifold with good transversal stability properties, and whose transversal dynamics governs the abrupt transition to synchronized behavior which has been observed in many other spatially extended chaotic systems.

Acknowledgements

This work was made possible by partial financial support from the following Brazilian government agencies: CNPq, CAPES and FINEP. The numerical computations were performed in the NAUTILUS cluster of the Universidade Federal do Paraná.

References

[1] J.P. Crutchfield, K. Kaneko, in: H.B. Lin (Ed.), Directions in Chaos, vol. 1, World Scientific, Singapore, 1987.
[2] K. Kaneko, in: K. Kaneko (Ed.), Theory and Applications of Coupled Map Lattices, Wiley, Chichester, 1993.
[3] K. Kaneko, Physica D 23 (1986) 436;
K. Kaneko, Physica D 34 (1989) 1.
[4] K. Kaneko, Physica D 41 (1990) 137.
[5] G. Paladin, A. Vulpiani, J. Phys. A 25 (1994) 4511;
A. Torcini, S. Lepri, Phys. Rev. E 55 (1997) R3805;
S.E. de S. Pinto, R.L. Viana, Phys. Rev. E 61 (2000) 5154.
[6] D.J. Watts, S.H. Strogatz, Nature 393 (1998) 440.
[7] M.E.J. Newman, D.J. Watts, Phys. Lett. A 263 (1999) 341;
M.E.J. Newman, D.J. Watts, Phys. Rev. E 60 (1999) 7332;
M.E.J. Newman, J. Stat. Phys. 101 (2000) 819.
[8] A.M. Batista, S.E. de S. Pinto, R.L. Viana, S.R. Lopes, Physica A 322 (2003) 118.
[9] H. Hong, M.Y. Choi, B.J. Kim, Phys. Rev. E 65 (2002) 26139.
[10] C. Li, G. Chen, Physica A 341 (2004) 73.
[11] A. Motter, C. Zhou, J. Kurths, Phys. Rev. E 71 (2005) 16116.
[12] H. Chaté, P. Manneville, Chaos 2 (1992) 307.
[13] P. Gade, Phys. Rev. E 54 (1996) 64.
[14] F.M. Atay, J. Jost, A. Wende, Phys. Rev. Lett. 94 (2004) 144101.
[15] M. Pineda, M.G. Cosenza, Phys. Rev. E 71 (2005) 057201.
[16] Y. Kuramoto, Chemical Oscillations, Waves, and Turbulence, Springer, Berlin, 1984;
H. Sakaguchi, S. Shinomoto, Y. Kuramoto, Prog. Theor. Phys. 77 (1987) 1005.
[17] H. Chaté, P. Manneville, Phys. Rev. Lett. 58 (1987) 112;
H. Chaté, P. Manneville, Physica D 32 (1988) 409;
H. Chaté, Europhys. Lett. 21 (1993) 419.
[18] A.M. Batista, S.E. de S. Pinto, R.L. Viana, S.R. Lopes, Phys. Rev. E 65 (2002) 056209.
[19] R.L. Viana, C. Grebogi, S.E. de S. Pinto, S.R. Lopes, A.M. Batista, J. Kurths, Phys. Rev. E 68 (2003) 067204.
[20] H. Fujisaka, T. Yamada, Prog. Theor. Phys. 70 (1983) 1240;
V.S. Afraimovich, N.N. Verichev, M.I. Rabinovich, Radiophys. Quantum Electron. 29 (1986) 795;
L. Pecora, T.S. Carroll, Phys. Rev. Lett. 64 (1990) 821.

[21] J. Milnor, Commun. Math. Phys. 99 (1985) 177.
[22] M. Hasler, Y.L. Maistrenko, IEEE Trans. Circuits Syst. 44 (1997) 856.
[23] P. Ashwin, J. Buescu, I. Stewart, Phys. Lett. A 193 (1994) 126.
[24] C. Anteneodo, S.E.S. Pinto, A.M. Batista, R.L. Viana, Phys. Rev. E 68 (2003) 045202(R);
Erratum: C. Anteneodo, S.E.S. Pinto, A.M. Batista, R.L. Viana, Phys. Rev. E 69 (2004) 045202 (E);
C. Anteneodo, A.M. Batista, R.L. Viana, Phys. Lett. A 326 (2004) 227.
[25] C. Grebogi, E. Ott, J.A. Yorke, Phys. Rev. Lett. 48 (1982) 1507.